2024 IEEE International Conference on Robotics and Automation (ICRA 2024)
May 13-17, 2024. Yokohama, Japan

In-Hand Rolling Manipulation Based on Ball-on-Cloth System

Hinano Ichikura and Mitsuru Higashimori

***Abstract*— This paper presents a novel in-hand rolling manipulation method in which a ball on a cloth attached to fingertips is controlled using flexible and adaptive deformation of the cloth. First, an analytical model of the ball-on-cloth system is introduced. The shape of the cloth is simplified, and the rolling constraint of the ball on the cloth is defined focusing on the lowest point of the ball. Next, the relationship between the input to the cloth anchor point and the position of the lowest point of the ball is expressed by a linear approximation. Then, the input to generate the desired rolling orbit is designed. Next, as an example of utilizing the rolling orbits, a manipulation method to rotate the ball around a vertical axis is developed. Finally, a multi-fingered hand with a piece of cloth attached to the fingertips is developed, and the effectiveness of the proposed system is experimentally verified.**

I. Introduction

Robotic manipulation is a topic of significant research interest [1]. Among manipulation techniques, in-hand manipulation, which controls the position and posture of an object within the hand, is expected to improve dexterity [2]. In-hand manipulation comprises two tasks: holding the object stably in the hand and giving the object translational and/or rotational motion. To perform in-hand manipulation, several approaches have been proposed, such as using a human-like multi-fingered hand [3]–[6], implementing special mechanisms such as rollers or crawlers on the fingers [7]–[12], and leveraging external environments, e.g., floors, walls, and gravity [13]–[15]. Fig. 1(a) shows a scenario of handling an object directly with the fingertips of a multi-fingered hand according to the above first approach "using a human-like multi-fingered hand." In this case, the finger posture of the hand must be changed actively to adapt to the shape, position, and posture of the object. Furthermore, to perform continuous manipulation, repositioning of the fingers is required. Further, as shown in Fig. 1(b), we consider attaching a cloth to the hand. This approach is classified as the second approach "to implement special mechanisms". The use of flexible materials such as cloth or rope for fingers and palms improves contact stability due to their high adaptability [16]–[19]. In Fig. 1(b), adaptive deformation of the cloth allows the object on the cloth to be held stably. Furthermore, the displacement of the fingertip changes the shape of the cloth and generates rolling and slipping of the object. In this study, we discuss an in-hand manipulation method using cloth.

In particular, we focus on the rolling manipulation of a spherical object. Rolling is an effective element for in-hand manipulation because it continuously changes the relative position and posture of the object in contact. As a manipulation problem considering rolling constraints, a ball-plate problem of controlling a rigid ball between two rigid plates (Fig. 2(a)) has been discussed [20]–[22]. There is a single contact point between the ball and plate, and the rolling is described as a nonholonomic constraint. One of the goals of the ball-plate problem is to control the posture of the ball by providing the rolling trajectory, i.e., displacement input to the upper plate (Fig. 2(c) upper row). Following the ball-plate problem, let us consider a "ball-on-cloth problem," which manipulates the ball on the cloth (Fig. 2(b)). In this problem, the cloth is in surface contact with the ball. When the contact area moves, both slipping and non-slipping areas may be generated. Thus, the ball-on-cloth problem is more complex and diverse than the ball-plate problems in terms of contact states. If the rolling of the ball on the cloth can be

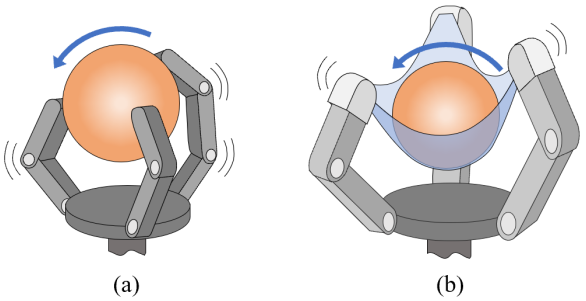

Fig. 1. Three-dimensional in-hand manipulation. (a) Multi-fingered hand. (b) Hand with a flexible cloth attached to the fingertips.

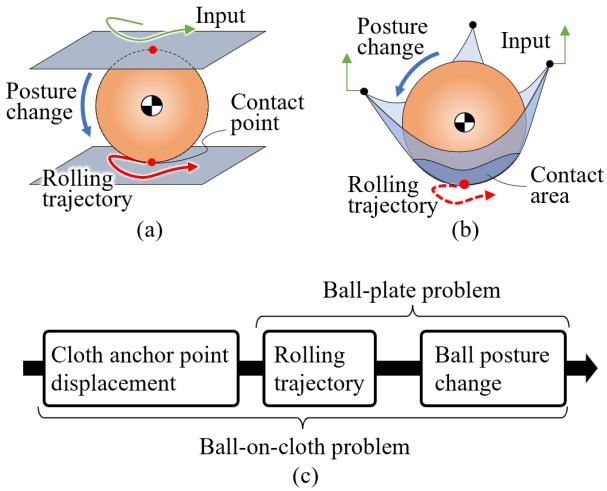

Fig. 2. In-hand manipulation utilizing rolling. (a) Ball-plate problem. (b) Ball-on-cloth problem. (c) Process flow.

*This work was not supported by any organization

The authors are with the Department of Mechanical Engineering, Graduate School of Engineering, Osaka University, Suita 565-0871, Japan. ichikura@ims.mech.eng.osaka-u.ac.jp; higashi@mech.eng.osaka-u.ac.jp

adequately represented, the manipulation method in the ball-plate problem is expected to be applicable (Fig. 2(c) lower row). Therefore, the goals of the ball-on-cloth problem are to represent a rolling trajectory for the input to the cloth anchor point and to solve the forward/inverse problem in its relationship.

In this paper, we discuss in-hand manipulation using a cloth. As shown in Fig. 1(b), an in-hand manipulation method comprising multi-fingered hand with a cloth attached to the fingertips to control the rolling trajectory of the ball on the cloth is presented. First, an analytical model of the ball-on-cloth system is introduced. The shape of the cloth is simplified, and rolling of the ball on the cloth is defined by the rolling constraint focused on the lowest point of the ball. Next, the relationship between the input to the cloth anchor point and the position of the lowest point of the ball is established. The relationship is approximated by a linear equation using numerical examples. The input to the cloth anchor point to control the position of the lowest point of the ball is designed. Next, the rotational manipulation method of the ball is discussed. Based on one of the orbit planning methods of the ball-plate problem [20], the input to the cloth anchor point is designed to rotate the ball around a vertical axis. Finally, a hand was developed and the effectiveness of the proposed method was experimentally verified. The control of the rolling trajectory and rotational manipulation of the ball were performed.

II. Ball-on-Cloth System

A. Modelling

Fig. 3(a) shows a three-dimensional analytical model of the ball-on-cloth system where a ball is placed on a cloth. The shape of the cloth is an equilateral triangle. The cloth is attached between the three fingers, connecting its vertices to the fingertips (hereafter called the cloth anchor points). The vertical positions of the cloth anchor points are controlled, while the horizontal positions are maintained constant. The ball is a rigid body with a uniform mass distribution. Fig. 3(b) shows a two-dimensional coordinate system for the position of the contact area of the ball as seen from the cloth (hereafter called the cloth coordinate system). The meanings of the symbols in Fig. 3 are as follows.

- Σ Base coordinate system. The xy-plane is horizontal and the z-axis is vertical.
- Σ_{ball} The coordinate system fixed to the ball. The origin is located at the center of the ball. The directions of the x_{ball}-, y_{ball}- and z_{ball}- axes in the initial state correspond to the directions of the x-, y- and z-axes in Σ.
- Σ_{cloth} Cloth coordinate system. The coordinate system is two-dimensional and represents the plane of the cloth when it is unfolded. The origin is located at the geometric center, and the directions of the X_{cloth}- and Y_{cloth}- axis correspond to the directions of the x- and y- axis in Σ.
- a Horizontal distance between the three anchor points of cloth in Σ.

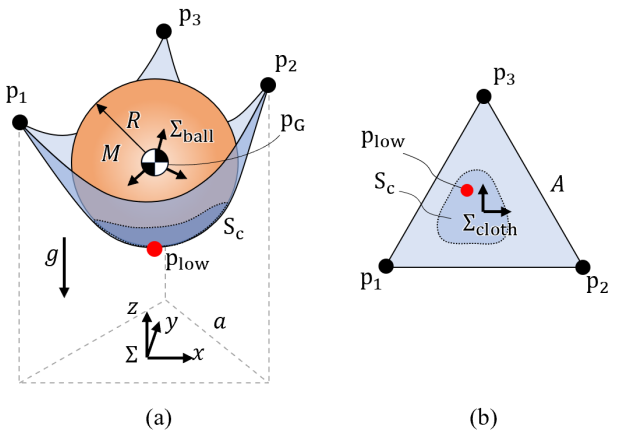

Fig. 3. Analytical model. (a) Absolute coordinate system. (b) Cloth coordinate system.

- A Length of one side of the cloth, i.e., distance between the three anchor points of the cloth in Σ_{cloth}.
- p_i Anchor point of the cloth ($i = 1, 2, 3$).
- $\boldsymbol{x}_i$ Position vector of p_i in Σ. $\boldsymbol{x}_i = [x_i, y_i, z_i]^T$ is given as follows:

$$\boldsymbol{x}_1 = \begin{bmatrix} -\frac{a}{2} \\ -\frac{\sqrt{3}a}{6} \\ z_1 \end{bmatrix}, \quad \boldsymbol{x}_2 = \begin{bmatrix} \frac{a}{2} \\ -\frac{\sqrt{3}a}{6} \\ z_2 \end{bmatrix}, \quad \boldsymbol{x}_3 = \begin{bmatrix} 0 \\ \frac{\sqrt{3}a}{3} \\ z_3 \end{bmatrix}. \tag{1}$$

- $\boldsymbol{X}_i$ Position vector of p_i in Σ_{cloth}. $\boldsymbol{X}_i = [X_i, Y_i]^T$ is given as follows:

$$\boldsymbol{X}_1 = \begin{bmatrix} -\frac{A}{2} \\ -\frac{\sqrt{3}A}{6} \end{bmatrix}, \quad \boldsymbol{X}_2 = \begin{bmatrix} \frac{A}{2} \\ -\frac{\sqrt{3}A}{6} \end{bmatrix}, \quad \boldsymbol{X}_3 = \begin{bmatrix} 0 \\ \frac{\sqrt{3}A}{3} \end{bmatrix}. \tag{2}$$

- R Radius of the ball.
- M Mass of the ball.
- p_{G} Center of the ball.
- $\boldsymbol{x}_{\mathrm{G}}$ Position vector of p_{G} in Σ. $\boldsymbol{x}_{\mathrm{G}} = [x_{\mathrm{G}}, y_{\mathrm{G}}, z_{\mathrm{G}}]^T$.
- $\boldsymbol{\theta}_{\mathrm{G}}$ Euler angle of the z-y-x system (intrinsic rotation) representing the orientation of Σ_{ball} in Σ. $\boldsymbol{\theta}_{\mathrm{G}} = [\theta_{\mathrm{G}x}, \theta_{\mathrm{G}y}, \theta_{\mathrm{G}z}]^T$.
- $\mathrm{p}_{\mathrm{low}}$ The lowest point of the ball in Σ. The position vector of $\mathrm{p}_{\mathrm{low}}$ in Σ is $\boldsymbol{x}_{\mathrm{low}} = [x_{\mathrm{G}}, y_{\mathrm{G}}, z_{\mathrm{G}} - R]^T$.
- $\boldsymbol{X}_{\mathrm{c}}$ Position vector of $\mathrm{p}_{\mathrm{low}}$ in Σ_{cloth}.
- S_{c} Contact area between the cloth and the ball.
- g Magnitude of gravitational acceleration.

To simplify the analysis, we employ the following assumptions.

1) The mass of the cloth, viscoelasticity in the bending direction, and deformation in the stretching direction are negligible. The cloth is freely deformable only in the bending direction.

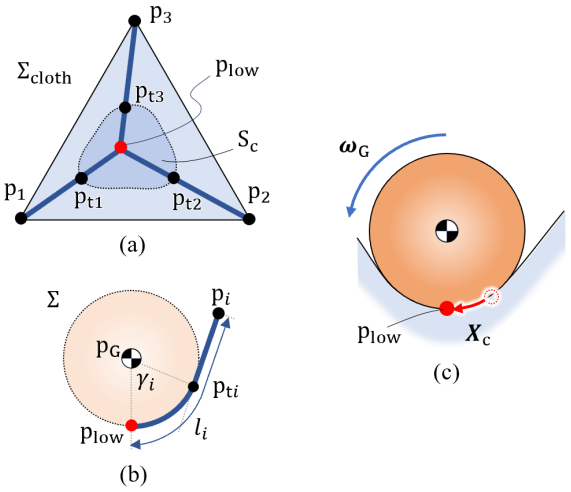

Fig. 4. Simplified analytical model. (a) Contact area in the cloth coordinate system. (b) Shape of the cloth. (c) Rolling of the ball on the cloth.

2) The lowest point of the ball is always in contact with the cloth.
3) The cloth is always under tension.
4) No wrinkles occur at the contact area of the cloth.

B. Simplified expression of the shape of the cloth

Practically, the cloth has infinite degrees of freedom and complex deformations with loosening and tension. In this study, the shape of the cloth is simplified as a representation with fewer variables. As shown in Fig. 4(a), a point p_{ti} is defined as the intersection of the line segment $\mathrm{p}_{\mathrm{low}}\mathrm{p}_i$ and the edge of the contact area S_c in Σ_{cloth}. The shape characteristics of the cloth in Σ are expressed as follows.

(i) The shape of the cloth in S_c is the same as the ball in Σ.
(ii) The shape of the cloth on the line segment $\mathrm{p}_{ti}\mathrm{p}_i$ in Σ_{cloth} is straight in Σ.

Based on (i) and (ii), the shape of the cloth in Σ is simplified using the curves p_i-p_{ti}-$\mathrm{p}_{\mathrm{low}}(i = 1, 2, 3)$ as shown in Fig. 4. Note that the four points p_i, p_G, $\mathrm{p}_{\mathrm{low}}$, and p_{ti} are supposed to be in the same vertical plane. Each curve comprises the line segment $\mathrm{p}_i\mathrm{p}_{ti}$ and arc $\mathrm{p}_{ti}\mathrm{p}_{\mathrm{low}}$. Let l_i denote the length of the curve and γ_i denote the angle between the line $\mathrm{p}_\mathrm{G}\mathrm{p}_{ti}$ and the z-axis. Let $\boldsymbol{l} = [l_1, l_2, l_3]^T$ and $\boldsymbol{\gamma} = [\gamma_1, \gamma_2, \gamma_3]^T$ be the vectors summarized for the curves $i = 1, 2, 3$ for l_i and γ_i, respectively. l_i is expressed as follows:

$$l_i = |\boldsymbol{X}_i - \boldsymbol{X}_\mathrm{c}|. \tag{3}$$

C. Definition of the rolling

In the ball-plate system, there is a single contact point between the ball and plate. When the ball rolls on the plate without slipping, the following rolling constraint holds between the velocity of the contact point on the plate $\boldsymbol{v}$ and the angular velocity vector of the ball $\boldsymbol{\omega}_\mathrm{G}$:

$$\boldsymbol{v} = -\boldsymbol{\omega}_\mathrm{G} \times \boldsymbol{r}, \tag{4}$$

where $\boldsymbol{r}$ is a vector from the center of the ball to the contact point. In this paper, we attempt to adapt (4) to the rolling in the ball-on-cloth system. We regard the lowest point of the ball $\mathrm{p}_{\mathrm{low}}$ as a representative point of the contact area, and the rolling constraint of the ball-on-cloth system is defined as follows:

$$\begin{bmatrix} \dot{\boldsymbol{X}}_\mathrm{c} \\ 0 \end{bmatrix} = -\boldsymbol{\omega}_\mathrm{G} \times \begin{bmatrix} 0 \\ 0 \\ -R \end{bmatrix}. \tag{5}$$

Note that the cloth is in surface contact with the ball. Verification of the effect of this approximation is a subject of future work. Hereafter, we assume that the rolling on the cloth, i.e., the rolling constraint at the lowest point of the ball $\mathrm{p}_{\mathrm{low}}$ is always satisfied. In this case, the friction coefficient between the ball and the cloth needs to be large and the velocity of $\boldsymbol{X}_\mathrm{c}$ needs to be small. These limitations are beyond the scope of this paper's discussion.

III. Cloth Anchor Point Displacement and Rolling Trajectory

A. Formulation of the geometry of the ball-on-cloth system under static conditions

From Figs. 4(a) and (b), the following constraints hold at each anchor point of the cloth ($i = 1, 2, 3$):

$$\boldsymbol{G}(\boldsymbol{q}) = [G_1, \cdots, G_9]^T = \boldsymbol{0}, \tag{6}$$

where,

$$\begin{aligned} \boldsymbol{q} &= [\boldsymbol{X}_\mathrm{c}^T, \boldsymbol{x}_\mathrm{G}^T, \boldsymbol{l}^T, \boldsymbol{\gamma}^T]^T \\ G_i &= l_i - |\boldsymbol{X}_i - \boldsymbol{X}_\mathrm{c}| \\ G_{i+3} &= (l_i - R\gamma_i)\cos\gamma_i + R\sin\gamma_i \\ &\quad - \sqrt{(x_i - x_\mathrm{G})^2 + (y_i - y_\mathrm{G})^2} \\ G_{i+6} &= (l_i - R\gamma_i)\sin\gamma_i - R\cos\gamma_i - (z_i - z_\mathrm{G}). \end{aligned}$$

From (6), with respect to the heights of the cloth anchor points z_i, there exists a solution under static conditions, i.e., a solution with minimum potential energy $U = Mgz_\mathrm{G}$. In this case, the position of the lowest point of the ball $\boldsymbol{X}_{\mathrm{c}0}$ is expressed as follows:

$$\boldsymbol{X}_{\mathrm{c}0} = \left\{ \boldsymbol{X}_\mathrm{c} \,\middle|\, \boldsymbol{G}(\boldsymbol{q}) = \boldsymbol{0},\ \frac{\partial U}{\partial \boldsymbol{X}_\mathrm{c}} = 0 \right\}. \tag{7}$$

B. Linear relationship equation based on numerical solutions

In this study, we assume that the anchor point p_3 is fixed ($z_3 = 0$) and the anchor points p_1 and p_2 is controlled as a input $\boldsymbol{u} = [z_1, z_2]^T$. After formulating the relationship between $\boldsymbol{u}$ and $\boldsymbol{X}_{\mathrm{c}0}$, the problem of designing $\boldsymbol{u}$ to satisfy the desired $\boldsymbol{X}_{\mathrm{c}0}$, i.e., the ball-on-cloth inverse problem is discussed. Let the relationship between $\boldsymbol{u}$ and $\boldsymbol{X}_{\mathrm{c}0}$ be approximated by the following linear equation:

$$\boldsymbol{X}_{\mathrm{c}0} = k\boldsymbol{B}\boldsymbol{u}, \tag{8}$$

where, k is a scalar of proportional constant and $\boldsymbol{B}$ is a 2×2 transformation matrix. The parameters k and $\boldsymbol{B}$ are estimated by fitting the values $\boldsymbol{u}$ and $\boldsymbol{X}_{\mathrm{c}0}$ calculated using

TABLE I

RESULTS OF FITTING PARAMETERS OF THE LINEAR EQUATIONS.

	(a)	(b)	(c)	(d)
a [mm]	75	75	105	105
R [mm]	10	30	10	30
$\hat{k}$	0.77	0.72	0.94	0.90
$\hat{B}_{11}$	0.87	0.87	0.87	0.87
$\hat{B}_{12}$	−0.87	−0.87	−0.87	−0.87
$\hat{B}_{21}$	0.50	0.50	0.50	0.50
$\hat{B}_{22}$	0.50	0.50	0.50	0.50
$RMSE$ [mm]	0.70	0.69	1.04	1.17

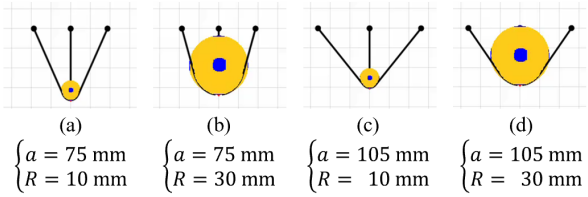

Fig. 5. Geometry of the ball-on-cloth system under static conditions.

(7). Table I shows the results of the fitting of k and $\boldsymbol{B}$, where $M = 0.1\,\mathrm{kg}$, $A = 150\,\mathrm{mm}$, $a = \{75, 105\}\,\mathrm{mm}$, $R = \{10, 30\}\,\mathrm{mm}$, $I = 36\,\mathrm{kg}\cdot\mathrm{mm}^2$. As the inputs, the range $-20 \le z_1 \le 20\,\mathrm{mm}$, $-20 \le z_2 \le 20\,\mathrm{mm}$, interval $4\,\mathrm{mm}$, and a total of 121 displacement inputs $\boldsymbol{u}$ are provided. Fig. 5 shows the geometry under static conditions when $z_1 = z_2 = 0\,\mathrm{mm}$. Note that we use the Levenberg-Marquardt algorithm [23] as the fitting method. As shown in Table I, $\hat{\boldsymbol{B}}$ is constant within two decimal places, regardless of the horizontal distance of the cloth anchor points a and radius of the ball R. $\hat{\boldsymbol{B}}$ can be approximated as follows:

$$\hat{\boldsymbol{B}} \approx \begin{bmatrix} \frac{\sqrt{3}}{2} & -\frac{\sqrt{3}}{2} \\ \frac{1}{2} & \frac{1}{2} \end{bmatrix}. \tag{9}$$

Moreover, as a increases and R decreases, $\hat{k}$ increases. Note that there may be no solution $\boldsymbol{X}_{\mathrm{c0}}$ when a and $|\boldsymbol{u}|$ are large relative to A. Fig. 6 shows the relationship between the values $\boldsymbol{X}_{\mathrm{c0}}$ (calculated by (7)) and the linear approximate solutions $\hat{\boldsymbol{X}}_{\mathrm{c}} = \hat{k}\hat{\boldsymbol{B}}\boldsymbol{u}$, where $a = 75\,\mathrm{mm}$, $R = 30\,\mathrm{mm}$. Where $|\boldsymbol{X}_{\mathrm{c0}}|$ is large, $\hat{\boldsymbol{X}}_{\mathrm{c}}$ deviates from $\boldsymbol{X}_{\mathrm{c0}}$. In contrast, for $|\boldsymbol{X}_{\mathrm{c0}}| \le 10\,\mathrm{mm}$, $\hat{\boldsymbol{X}}_{\mathrm{c}}$ is well matched to $\boldsymbol{X}_{\mathrm{c0}}$. Within this range, the approximate equation is valid. Therefore, as the input $\hat{\boldsymbol{u}}$ approximately satisfying the desired $\boldsymbol{X}_{\mathrm{c0}}$, we use the following equation:

$$\hat{\boldsymbol{u}} = \frac{1}{\hat{k}}\hat{\boldsymbol{B}}^{-1}\boldsymbol{X}_{\mathrm{c0}} \tag{10}$$

IV. ROTATIONAL MANIPULATION OF BALL

In this section, we discuss the control of the posture of the ball by giving $\boldsymbol{X}_{\mathrm{c}}$ as the input. The rotational manipulation method of the ball around the vertical axis (Fig. 7(a)) is developed using the circle-based path planning method proposed as an algorithm for the ball-plate problem [20]. As shown in Fig. 7(b), we assume that the ball rolls along the circular orbit closkwise along Σ_{cloth}. Let C denote the radius

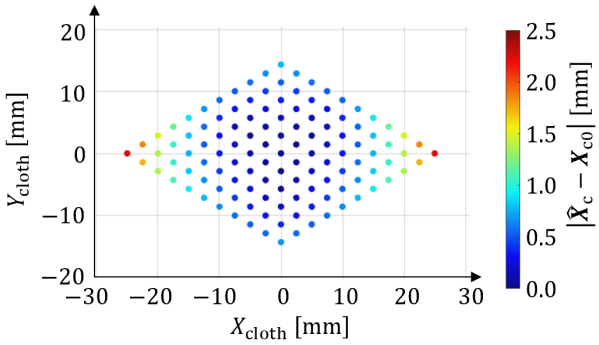

Fig. 6. Linear approximate solutions $\hat{\boldsymbol{X}}_{\mathrm{c}}$ and error of $\hat{\boldsymbol{X}}_{\mathrm{c}}$ with the calculated values $\boldsymbol{X}_{\mathrm{c0}}$.

of the orbit and f denote the frequency of the revolution. $\boldsymbol{X}_{\mathrm{c}}$ is expressed as follows:

$$\boldsymbol{X}_{\mathrm{c}} = [C\cos(2\pi ft), -C\sin(2\pi ft)]^T. \tag{11}$$

In this case, the orbit of the lowest point of the ball $\mathrm{p}_{\mathrm{low}}$ as viewed from Σ_{ball} (brown line in Fig. 7(b)) is a circular orbit with the radius R_{c}. R_{c} is expressed as follows:

$$R_{\mathrm{c}} = \frac{RC}{\sqrt{R^2 + C^2}}. \tag{12}$$

Let T denote a period of one revolution of the circular orbit. The posture change of the ball from t to $t+T$, is expressed as follows:

$$\boldsymbol{n}_{\mathrm{r}} = \frac{1}{\sqrt{C^2 + R^2}} \begin{bmatrix} C\cos(2\pi ft) \\ -C\sin(2\pi ft) \\ R \end{bmatrix} \tag{13}$$

$$\Delta\theta_{\mathrm{r}} = 2\pi\left(\frac{\sqrt{C^2 + R^2}}{R} - 1\right), \tag{14}$$

where $\boldsymbol{n}_{\mathrm{r}}$ is a vector of the rotation axis and $\Delta\theta_{\mathrm{r}}$ is the angle of the rotation. When the radius of the circular orbit is sufficiently smaller than the radius of the ball ($C \ll R$), from (13), the rotation axis is close to the z-axis ($\boldsymbol{n}_{\mathrm{r}} \approx [0, 0, 1]^T$). In this case, the ball revolving along the circular orbit clockwise is regarded as rotating around the vertical axis counterclockwise. Based on this planning method, the input to rotate the ball around the vertical axis counterclockwise at the target angular velocity ω_{target} is designed as follows. From (13) and (14), the target radius of the circular orbit C_{target} is expressed as follows:

$$C_{\mathrm{target}} = R\sqrt{\left(\frac{\omega_{\mathrm{target}}}{2\pi f}\right)^2 + 2\left(\frac{\omega_{\mathrm{target}}}{2\pi f}\right)}. \tag{15}$$

When f is small and quasi-static motion can be assumed, the input is designed by substituting (11) and (15) for (10), as follows:

$$\boldsymbol{u} = P\begin{bmatrix} \sin\left(2\pi ft + \frac{5}{6}\pi\right) \\ \sin\left(2\pi ft + \frac{7}{6}\pi\right) \end{bmatrix}, \tag{16}$$

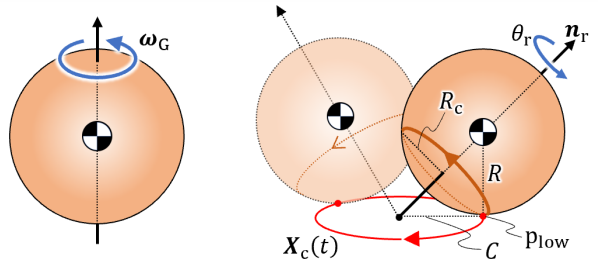

Fig. 7. Manipulation planning. (a) The desired rotation of the ball is around the vertical axis. (b) An equivalent rotation around the vertical axis is generated via a circular rolling orbit.

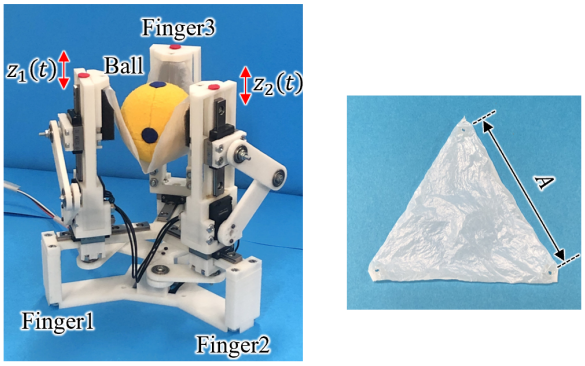

Fig. 8. Experimental system. (a) Three-fingered hand. (b) Cloth attached to the fingertips.

where,

$$P = \frac{2R}{\sqrt{3}\hat{k}}\sqrt{\left(\left(\frac{\omega_{\text{target}}}{2\pi f}\right)^2 + 2\left(\frac{\omega_{\text{target}}}{2\pi f}\right)\right)} \tag{17}$$

is the input amplitude. From (16) and (17), the input frequency f and the input amplitude P have a trade-off relationship with respect to ω_{target}. Practically, the range of P is limited by the mechanism of the hand and the size of the cloth. Moreover, as f increases, it becomes more likely that slipping between the cloth and ball occurs and the motion derivates from that of the analytical model.

V. Experiments

A. Experimental system

Fig. 8(a) and Fig. 9 show the hand developed for experimentation. The size of the hand is $H_1 = 124\,\text{mm}$, $H_2 = 63\,\text{mm}$, $W = 178\,\text{mm}$ and $D = 154\,\text{mm}$. The back finger is fixed and the two fingers in front are movable. The slider mechanisms are attached to the movable fingers (Fig. 9(a)), and a vertical displacement is provided to the fingertip using servo motors. Each finger is connected to the palm by a trident link mechanism (Fig. 9(b)), and the interval between the fingers is controlled in the range $35 \le a \le 105\,\text{mm}$. Between the three fingertips, the cloth with a side length $A = 150\,\text{mm}$ is attached (Fig. 8(b)). The object is a ball with radius $R = 30\,\text{mm}$ (Fig. 8(a)). The static and dynamic friction coefficients between the cloth and the ball

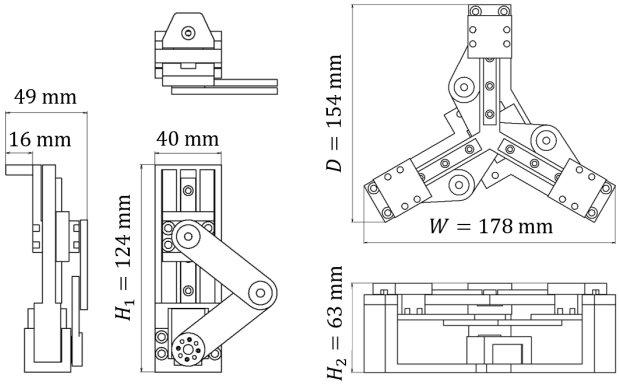

Fig. 9. Blueprint of the hand. (a) Finger mechanism. (b) Gripper mechanism.

are $\mu_s = 0.24$ and $\mu_d = 0.19$, respectively. A 6-axis inertial measurement unit (IMU) is embedded inside the ball to measure the posture of the ball $\boldsymbol{\theta}_G$.

B. Control of the orbit of the lowest point of the ball

Experiments were conducted to follow $\boldsymbol{X}_c$ to the target orbits. The target orbits $\boldsymbol{X}_{cr}$ were expressed as follows:

$$\text{(a)} \quad \begin{cases} X_{cr} &= 10\cos\phi\sin(2\pi ft)\,\text{mm} \\ Y_{cr} &= 10\sin\phi\sin(2\pi ft)\,\text{mm} \\ \phi &= \{0,\ \pi/6,\ \pi/3,\ \pi/2\}\ \text{rad} \end{cases} \tag{18}$$

$$\text{(b)} \quad \begin{cases} X_{cr} &= 10\sin(2\pi ft - \pi/2)\,\text{mm} \\ Y_{cr} &= 10\eta\sin(2\pi ft)\,\text{mm} \\ \eta &= \{1/3,\ 2/3,\ 1,\ 4/3\} \end{cases} \tag{19}$$

$$\text{(c)} \quad \begin{cases} X_{cr} &= 10\sin(2\pi\kappa ft - \pi/2)\,\text{mm} \\ Y_{cr} &= 10\sin(2\pi ft)\,\text{mm} \\ \kappa &= \{1/2,\ 2/3,\ 3/2,\ 2\} \end{cases} . \tag{20}$$

Fig. 10 shows the experimental results, where the interval of the fingers was $a = 75\,\text{mm}$ and the input frequency was $f = 0.5\,\text{Hz}$. Note that we assume that the rolling constraint in (5) and quasi-static conditions are maintained. In this assumption, the experimental values of the lowest point of the ball $\boldsymbol{X}_{ce}$ were calculated by substituting the angular velocity $\boldsymbol{\omega}_G$ (obtained by the IMU at interval $\Delta t = 0.02\,\text{s}$) into the following equation:

$$\boldsymbol{X}_{ce}(t+\Delta t) = \boldsymbol{X}_{ce}(t) + R\Delta t \begin{bmatrix} \omega_{Gy} \\ -\omega_{Gx} \end{bmatrix}, \tag{21}$$

where, $\boldsymbol{X}_{ce}(0) = [0,0]^T$. As shown in Fig. 10, the experimental values $\boldsymbol{X}_{ce}$ were fully matched with the target values $\boldsymbol{X}_{cr}$. The error average was $\overline{|\boldsymbol{X}_{cr} - \boldsymbol{X}_{ce}|} = 2.62\,\text{mm}$, and thus, the effectiveness of the control method of the rolling orbit was confirmed.

C. Rotational manipulation of the ball

A counterclockwise rotational manipulation around the vertical axis of the ball was performed with the target angular velocity $\omega_{\text{target}} = 10°/\text{s}$. Setting the input frequency to $f = 0.5\,\text{Hz}$, we obtain $z_1 = 16.3\sin(\pi t - \pi/3)\,\text{mm}$, $z_2 = 16.3\sin(\pi t)\,\text{mm}$ as the input from (16). In this

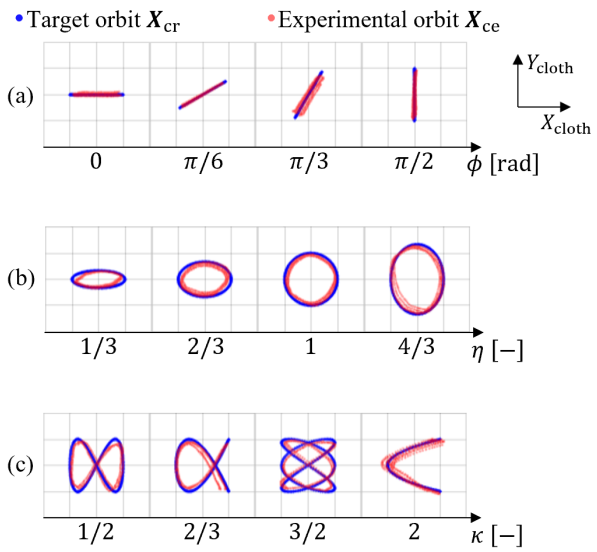

Fig. 10. Results of control of the rolling orbit.

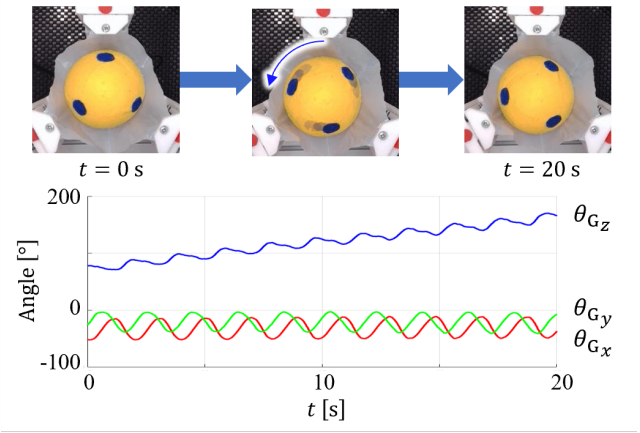

Fig. 11. Results of rotational manipulation around the vertical axis.

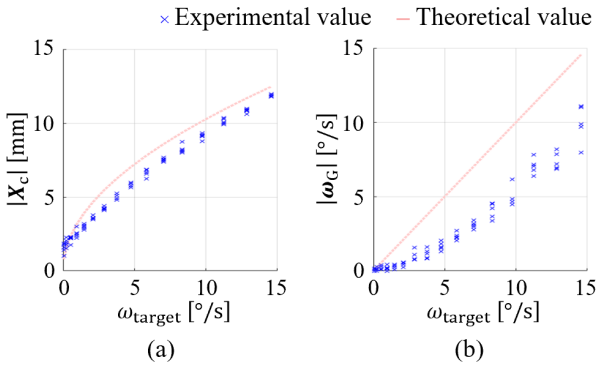

Fig. 12. Experimental results of the rotational manipulation. (a) Radius of the circular orbit. (b) Magnitude of the angular velocity.

case, the theoretical values of the posture change in four cycles (i.e. 8 seconds) is the rotational axis $\boldsymbol{n}_r = [0.32\cos\psi, 0.32\sin\psi, 0.95]^T$ and the angle of rotation $\Delta\theta_r = 80°$. Fig. 11 shows the experimental results. The parameters other than the input were the same as those in Fig. 10. As shown in Fig. 11, θ_{Gx} and θ_{Gy} oscillated around constant values, while θ_{Gz} increased periodically. The experimental value of the posture change in four cycles was $\boldsymbol{n}_r = [0.16, -0.33, 0.93]^T$, $\Delta\theta_r = 36°$ (the average angular velocity $\overline{|\boldsymbol{\omega}_G|} = \Delta\theta_r f/4 = 4.5°/s$).

Next, we conducted experiments on the vertical axis counterclockwise rotational manipulation, where the target angular velocity was $0.06 \leq \omega_{target} \leq 15°/s$. Figs. 12(a) and (b) show the radius of the lowest point of the ball $|\boldsymbol{X}_c|$ and the magnitude of the angular velocity of the ball $|\boldsymbol{\omega}_G|$, respectively. Five experiments were conducted on each target angular velocity. The theoretical values of $|\boldsymbol{X}_c|$ were obtained from (15). As shown in Fig. 12, the experimental values of $|\boldsymbol{X}_c|$ are slightly smaller than the theoretical values, while the experimental values of $|\boldsymbol{\omega}_G|$ are significantly smaller than the theoretical values. The factors for these differences are considered to be the viscosity of the cloth in the bending direction and energy dissipation due to micro slip on the contact surface between the cloth and the ball, both of which are ignored in the analytical model. However, the theoretical values and experimental values are in qualitative agreement, thus confirming the feasibility of the proposed method.

VI. Conclusion

In this paper, we discussed an in-hand manipulation using a cloth. The main results are summarized as follows.

- Based on an analytical model of a ball-on-cloth system, a simplified geometry of the cloth and rolling constraints of the ball were defined.
- The relationship between the cloth anchor points and the lowest point of the ball was established. A solution method for designing an input to the cloth anchor points to satisfy the desired orbit of the lowest point of the ball was developed.
- As a manipulation method for a ball, a method that rotates the ball around the vertical axis by providing an input to the cloth anchor points was constructed.
- A multi-fingered hand with a piece of the cloth attached was developed, and the effectiveness of the proposed method was experimentally verified.

In the ball-plate problem, more variations of rolling trajectory allow for rotation around various axes. On the other hand, in the ball-on-cloth problem, a rolling trajectory is limited by the area of the cloth, and the achievable rotations are smaller and slower. Therefore, to achieve a variety of rotational manipulations, it is necessary to utilize dynamic motion including slipping. Future work will include discussions about manipulation problems utilizing the high adaptability of the cloth where the shape of the object is not spherical. Furthermore, extensions to analyses of contact force distribution between the cloth and object should be discussed. Beyond control of the position and the posture of the object, we would like to develop a discussion of the problem of controlling a shape of a soft object.

REFERENCES

[1] T. Watanabe, K. Yamazaki and Y. Yokokohji: "Survey of robotic manipulation studies intending practical applications in real environments -object recognition, soft robot hand, challenge program and benchmarking-," Adv. Robot., vol. 31, no. 19-20, pp. 1114–1132, 2017.

[2] I. M. Bullock, R. R. Ma, and A. M. Dollar: "A hand-centric classification of human and robot dexterous manipulation," IEEE Trans. Haptics, vol. 6, no. 2, pp. 129–144, 2013.

[3] G. Solak and L. Jamone: "Learning by demonstration and robust control of dexterous in-hand robotic manipulation skills," Proc. of IEEE/RSJ Int. Conf. Intell. Robots Syst., pp. 8246–8251, 2019.

[4] OpenAI et al.: "Learning dexterous in-hand manipulation," 2019. [Online]. Available: https://openai.com/blog/learning-dexterity/

[5] J. Zhou, J. Yi, X. Chen, Z. Liu, and Z. Wang: "BCL-13: A 13- DOF soft robotic hand for dexterous grasping and in-hand manipulation," IEEE Robot. Automat. Lett., vol. 3, no. 4, pp. 3379–3386, 2018.

[6] A. S. Morgan, K. Hang, B. Wen, K. Bekris and A. M. Dollar: "Complex in-hand manipulation via compliance-enabled finger gaiting and multi-modal planning," IEEE Robot. Automat. Lett., vol. 7, no. 2, pp. 4821–4828, 2022.

[7] Y. Cai and S. Yuan: "In-hand manipulation in power grasp: design of an adaptive robot hand with active surfaces," in Proc. of 2023 IEEE Int. Conf. Robot. Automat., pp. 10296–10302, 2023.

[8] S. Yuan, L. Shao,C. L. Yako, A. Gruebele, and J. K. Salisbury: "Design and control of roller grasper V2 for in-hand manipulation," in Proc. IEEE/RSJ Int. Conf. Intell. Robots Syst., pp. 9151–9158, 2020.

[9] A. J. Spiers, A. S. Morgan, K. Srinivasan, B. Calli and A. M. Dollar: "Using a variable-friction robot hand to determine proprioceptive features for object classification during within-hand-manipulation," IEEE Trans. Haptics, vol. 13, issue. 3, pp. 600–610, 2020.

[10] R. R. Ma and A. M. Dollar: "In-hand manipulation primitives for a minimal, underactuated gripper with active surfaces," in Proc. ASME Int. Des. Eng. Tech. Conf., 2016, Art. no. V05AT07A072.

[11] S. Abondance, C. B. Teeple, and R. J. Wood: "A dexterous soft robotic hand for delicate in-hand manipulation," IEEE Robot. Automat. Lett., vol. 5, no. 4, pp. 5502–5509, 2020.

[12] H. Ichikura and M. Higashimori: "In-hand manipulation inspired by diabolo juggling," IEEE Robot. Automat. Lett., vol. 7, no. 4, pp. 12227–12234, 2022.

[13] N. C. Dalfe, A. Rodriguez, R. Paolini, B. Tang, S. S. Srinivasa, M. Erdmann, M. T. Mason, I. Lundberg, H. Staab and T. Fuhlbrigge: "Extrinsic dexterity: In-hand manipulation with external forces," in Proc. of 2014 IEEE Int. Conf. Robot. Automat., pp. 1578–1585, 2014.

[14] J. Shi, J. Z. Woodruff, P. B. Umbanhowar, and K. M. Lynch: "Dynamic in-hand sliding manipulation," IEEE Trans. Robot., vol. 33, no. 4, pp. 778–795, 2017.

[15] R. R. Ma, W. G. Bircher and A. M. Dollar: "Toward robust, whole-hand caging manipulation with underactuated hands," in Proc. IEEE Int. Conf. Robot. Automat., pp. 1336–1342, 2017.

[16] H. Iwamasa and S. Hirai: "Binding of food materials with a tension-sensitive elastic thread," Proc. IEEE Int. Conf. Robot. Automat., pp. 4298–4303, 2015.

[17] B. Donald, L. Gariepy, and D. Rus: "Distributed manipulation of multiple objects using ropes," Proc. IEEE Int. Conf.Robot.Automat., vol. 1, pp. 450–457, 2000.

[18] T. Maneewarn and P. Detudom: "Mechanics of cooperative nonprehensile pulling by multiple robots," Proc. IEEE/RSJ Int. Conf. Intell. Robots Syst., pp. 2004–2009, 2005.

[19] J. Buzzatto et al.: "Soft, multi-layer, disposable, kirigami based robotic grippers: On handling of delicate, contaminated, and everyday objects," Proc. IEEE/RSJ Int. Conf. Intell. Robots Syst., pp. 5440–5447, 2022.

[20] M. Svinin and S. Hosoe: "Motion planning algorithms for a rolling sphere with limited contact area," IEEE Trans. Robot., vol. 24, issue 3, pp. 612–625, 2008.

[21] G. Oriolo, M. Vendittelli, A. Marigo and A. Bicchi: "From nominal to robust planning: the plate-ball manipulation system," Proc. IEEE Int. Conf. Robot. Automat., pp. 3175–3180, 2005.

[22] H. Date, M. Sampei, M. Ishikawa and M. Koga: "Simultaneous control of position and orientation for ball-plate manipulation problem based on time-state control form," IEEE Trans. Robot. Automat., vol. 20, issue 3, pp. 465–480, 2004.

[23] T. Sugihara: "Solvability-unconcerned inverse kinematics by the levenberg-marquardt method," IEEE Trans. Robot., vol. 27 no. 5, pp. 984–991, 2011.